Observations of the phases of the substorm

I. O. Voronkov
Department of Physics, University of Alberta, Edmonton, Alberta, Canada

E. F. Donovan
Department of Physics and Astronomy, University of Calgary, Calgary, Alberta, Canada

J. C. Samson
Department of Physics, University of Alberta, Edmonton, Alberta, Canada

Received 5 February 2002; revised 27 June 2002; accepted 12 December 2002; published 12 February 2003.

[1] Following the database of large-scale vortices during pseudo-breakup and breakup registered by the Gillam All-Sky Imager, we selected one event (19 February 1996) for a detailed consideration. This event is a sequence of pseudo-breakup and local substorm, and breakup followed by the large substorm, which is isolated from the previous pseudo-breakup by the second growth phase. Commencement of these elements of auroral activity was clearly seen above the Churchill line of the Canadian Auroral Network for the OPEN Program Unified Study (CANOPUS; pseudo-breakup was completely covered by the field of view of the Gillam All-Sky Imager). Geotail was located at $\sim$19 R_E in the equatorial plane of midnight sector, which, along with supporting observations from two geostationary satellites (GOES 8 and 9), allowed for a comparison of ground-based, geostationary orbit and midtail signatures. The pseudo-breakup consisted of two distinct stages: a near-exponential arc intensity growth and a poleward vortex expansion that started simultaneously with dipolarization in the inner magnetosphere. The latter corresponded to explosive onset of short-period (tens of millihertz) pulsations observed at geostationary orbit and on the ground in the vicinity of the arc. No significant disturbances poleward of the vortex were observed. Pseudo-breakup was followed by the second growth phase, which involved a significant thinning of the plasma sheet. Breakup was of a similar two-stage character as the pseudo-breakup. Full onset of the expansive phase that followed breakup was seen simultaneously by all instruments including Geotail, which detected strong perturbations in the midtail. The expansive phase onset launched the second postbreakup package of Pi2 pulsations that were of larger amplitude. Finally, during the substorm recovery phase, the poleward boundary intensifications (PBIs) were observed as long-period, on the order of 10 min, pulses of electron precipitation. PBI commencement coincided with bursty flows and pulses of plasma energization in the midtail. Observed features support recent ideas claiming that we are dealing with processes (breakup, full onset of the expansive phase, and PBIs) of a distinct physical nature that require different commencement thresholds, namely, the inner plasma sheet instability (pseudo-breakup and breakup), midtail reconnection (expansive phase onset), and further magnetotail dynamics during the recovery phase (PBIs). *INDEX TERMS:* 2704 Magnetospheric Physics: Auroral phenomena (2407); 2788 Magnetospheric Physics: Storms and substorms; 2407 Ionosphere: Auroral ionosphere (2704); 2764 Magnetospheric Physics: Plasma sheet

Citation: Voronkov, I. O., E. F. Donovan, and J. C. Samson, Observations of the phases of the substorm, *J. Geophys. Res.*, *108*(A2), 1073, doi:10.1029/2002JA009314, 2003.

1. Introduction

1.1. General

[2] The phenomenological definition of the magnetospheric substorm is based on observations of auroral and magnetospheric processes [e.g., *Akasofu*, 1977]. The entire process involves a growth phase, breakup, expansive phase, and recovery phase. During the growth phase, the auroral distribution moves equatorward, convection enhances, and the magnetospheric magnetic field topology at the night side becomes stretched. Immediately preceding the breakup, a discrete auroral arc that is within the proton aurora intensifies. The breakup and substorm onset involve both the

0148-0227/03/2002JA009314$09.00

Table 1. Stages of Substorm

Stage	Ground-Based Observable Features	Duration	Underlying Physics
Growth phase	- Equatorward motion of the proton aurora; - Proton aurora brightening; - Convection and electrojet enhancement.	tens of minutes	energy storage
Arc intensification	- brightening of an equatorward arc.	minutes	not known
Breakup or Pseudo-breakup	- Vortex formation; - Vortex poleward expansion; - Poleward motion of the proton aurora.	tens of seconds to minutes	energy release
Full onset and expansive phase	- Poleward expansion of the electron aurora; - Westward travelling surge; - Large amplitude westward electrojet.	tens of minutes	NENL
Recovery phase	- Equatorward retreat of electron aurora; - Substorm electrojet fading; - Poleward boundary intensifications; - Morning sector auroras.	tens of minutes	relaxation

development of that arc into a vortex structure, a poleward expansion of the vortex within the auroral oval, the dipolarization (i.e., relaxation) of the magnetic field topology in the inner central plasma sheet (CPS), the energization of CPS plasma, and the magnetic signature of enhanced ionospheric currents. In the expansive phase, the expanding vortex reaches the poleward boundary of diffuse electron precipitation, which in turn also expands poleward. The expansive phase lasts minutes to tens of minutes, after which the system returns to a less disturbed state during the recovery phase, which lasts tens of minutes.

[3] A picture of the substorm as a dynamic sequence of energy storage and release in the magnetotail has evolved basing primarily on this phenomenology. The growth phase is a period of energy storage in both the magnetotail magnetic field and CPS plasma. This energy is extracted from the solar wind through enhanced merging on the dayside. On the basis of statistical studies, it has been argued that the breakup is triggered by an interruption of this energy storage that results from, for example, a northward turning of the interplanetary magnetic field (IMF) [e.g., *Lyons et al.*, 1997]. The intensification, dipolarization, and enhanced ionospheric currents are all related to a diversion of magnetotail current through the ionosphere, and a release of energy stored in the stretched magnetic field topology. In Table 1, we list the stages of the substorm relevant to this paper, selected ground-based observations typically associated with them, their characteristic time scales, and brief comments on the nature of the energy storage and/or release.

[4] Although the term ''pseudo-breakup'' is widely used in the literature, there is no uniformly accepted definition of the term. There is debate about whether or not the ''pseudo-breakup'' is different in any substantive way from a ''breakup'' [e.g., *Rostoker*, 1998]. This term is often applied to what have been called ''local'' or ''weak'' substorms [see, e.g., *Mishin et al.*, 2000, and references therein]. Following *Voronkov et al.* [2000a] we use the term pseudo-breakup to describe an auroral disturbance that results in the formation of a vortex that does not expand as far poleward as the polar cap boundary, and that is not accompanied by signatures of lobe flux reconnection. From our perspective, both breakups and pseudo-breakups begin with the intensification of a discrete auroral arc, and lead to vortex formation. Pseudo-breakups ''stall'' before lobe field lines are involved whereas breakups are followed by a full expansive phase onset presumably associated with lobe flux reconnection.

[5] The view of the substorm in terms of energy storage and release [*Rostoker et al.*, 1980; *Rostoker*, 1999] is still fundamentally phenomenological. Substorm models seek to explain the underlying plasma physical processes, such as the instability that leads to the breakup. The accepted framework of observational constraints was developed on the basis of data that is of lower resolution both temporally and spatially than is available today. For some aspects of the substorm problem, this poses no great difficulty. The growth phase, for example, is well characterized by relatively low resolution data [*McPherron*, 1970]. The same can almost certainly be said for the recovery phase, though it has been less thoroughly studied [e.g., *Opgenoorth et al.*, 1994]. On the other hand, expansive phase onset is an extremely fast and apparently local process [e.g., *Friedrich et al.*, 2001a, 2001b] characterized both in the magnetosphere and the ionosphere by significant morphological changes that occur on time scales of tens of seconds or even less. Additionally, difficulties in observing onset related phenomena are often exacerbated by significantly disturbed background conditions that can obscure the real commencement of breakup and expansive phase activity.

[6] There are two well developed models of the substorm onset process. These are the Near Earth Neutral Line (NENL) [e.g., *Hones*, 1979; *McPherron*, 1992; *Baker et al.*, 1996], and Current Disruption models [e.g., *Lui et al.*, 1988; *Ohtani et al.*, 1999]. Both are observationally based and incorporate auroral breakup at the equatorward edge of the auroral oval [*Akasofu*, 1977] and magnetotail disruption at $\sim$20–30 R_E [*Hones*, 1984]. The models differ in terms of where (both in space and time) breakup maps to the magnetosphere and where the reconnection region maps to the ionosphere, and how these regions are tied to one another. The difficulty in resolving the differences between the two views is a direct consequence of the historical lack of adequate high temporal and spatial resolution observations of the onset phenomena, both in situ and in terms of its ionospheric signatures. Clearly identifying and characterizing the sequence of events around substorm onset, with the goal of developing constraints for models of the involved physical processes, is one of central objectives in space physics research. To this

end, substorms which occur at times when there is a fortuitous arrangement of satellites and ground-based instruments are extremely valuable.

[7] In this paper, we present data from a period of substorm activity that occurred on 19 February 1996, during the period 0300 to 0700 UT. This event consisted of a well defined growth phase, pseudo-breakup, second growth phase, breakup, expansive phase, and recovery phase with poleward boundary intensifications. The sequence of substorm related phenomena was the only obvious activity during this time period. The preceding conditions were comparatively quiet and the substorm related perturbations were isolated with clearly identifiable stages. The onset related activity was localized in the local time sector of the Canadian Auroral Network for the OPEN Program Unified Study (CANOPUS) Churchill line of magnetometers. The viewing conditions overhead the CANOPUS optical instruments at Gillam and Rankin Inlet were excellent. GOES 8 and 9 were located on geosynchronous orbit, bracketing the Churchill meridian. Geotail was located near midnight at $\sim$19 R_E. Figure 1 is a map of Canada, showing the CANOPUS sites, and the footprints of the GOES 8 and 9, and Geotail spacecraft according to the T89 model [*Tsyganenko*, 1989].

[8] This study focuses on the ground-based and magnetospheric signatures for this particular event. Our primary objective is to identify and document a relatively clear sequence of ground based signatures, and to highlight aspects of the data that may suggest the location of these processes in the magnetosphere. Before we begin, we wish to review what we feel are the relevant published substorm observations.

1.2. Review of Relevant Observations

[9] We begin with a brief review of the recent studies of near-Earth and midtail processes at the expansive phase. Ground-based optical breakup starts from the most equatorward arc [*Akasofu*, 1977] that appears in the proton aurora region [*Samson et al.*, 1992], intensifies on a time scale of minutes [*Friedrich et al.*, 2001a, 2001b]. For several cases, L. R. Lyons et al. (Relation of a substorm breakup arc to other growth phase arcs, submitted to *Journal of Geophysical Research*, 2002, hereinafter referred to as Lyons et al., manuscript submitted, 2002) have found that this equatorward "breakup" arc is a new arc that appears right before breakup and is distinct from growth-phase arcs. This intensification is followed by the arc undulation [*Murphree and Johnson*, 1996] giving the start of large-scale vortex formation and its poleward expansion. Statistical analyses of optical signatures for this process in different optical wavelengths using high-resolution ground-based ASI and MSP observations showed an amazing recurrence of the arc position with respect to the proton aurora band and of the ratio of the arc thickness to the arc-aligned undulation wavelength [*Voronkov et al.*, 2000a]. Ground-based breakup is accompanied by significant variations of plasma parameters and magnetic field at the geostationary orbit. Observations in the inner plasma sheet show that a burst of short period, on the order of seconds to tens of seconds, magnetic pulsations [e.g., *Roux et al.*, 1991] and magnetic field dipolarization accompany the breakup. These observations were consistent with event

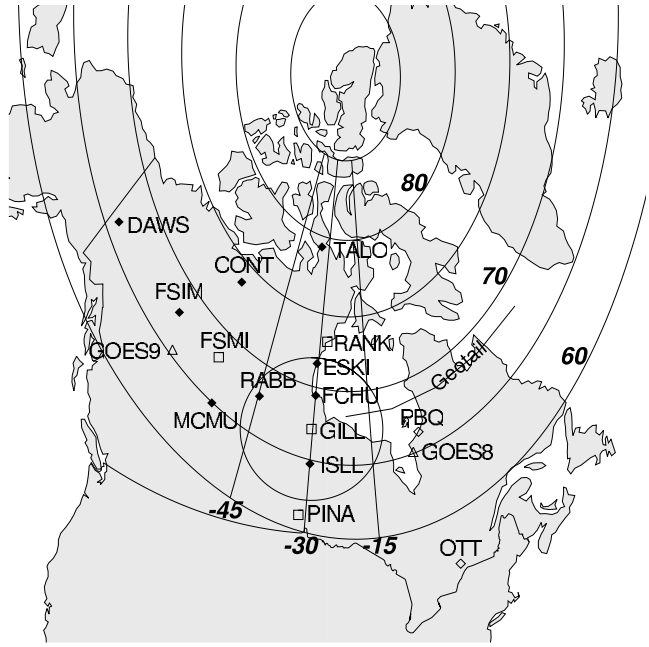

Figure 1. Schematic of the CANOPUS instruments used in this study. Notations are as follows. Grey diamonds: CANOPUS magnetometer sites Dawson (DAWS), Contwoyto Lake (CONT), Taloyoak (TALO), Fort Simpson (FSIM), Fort McMurray (MCMU), Rabbit Lake (RABB), Eskimo Point (ESKI), Fort Churchill (FCHU), and Island Lake (ISLL). Squares: CANOPUS sites with both magnetometers and Meridian Scanning Photometers (MSPs) Fort Smith (FSMI), Rankin Inlet (RANK), Gillam (GILL), and Pinawa (PINA). Transparent diamonds: NRCan magnetometers in Poste-de-la-Ballein (PBQ) and Ottawa (OTT). Triangles: footprints of positions of the geostationary satellites GOES 8 and GOES 9. The footprint of the Geotail trajectory is shown by the solid line. Mapping of the satellite positions was made using T89 model [*Tsyganenko*, 1989]. The circle shows the field of view of the Gillam ASI. Coordinate grid is PACE.

studies using spacecraft tailward of the geostationary orbit. Signatures of cross-tail current growth ("explosive growth phase" [*Ohtani et al.*, 1992]) and disruption [*Lui et al.*, 1988] followed by particle injections into the inner magnetosphere [*Reeves et al.*, 1992] and electromagnetic energy flux toward the ionosphere [*Maynard et al.*, 1996; *Erickson et al.*, 2000] were observed. The repeatability of, and correlation between, ground-based and near-geosynchronous satellite signatures of breakups allow for identification of their relationship in event studies. This is one of objectives of this paper.

[10] Alternatively, numerous midtail satellite observations, mainly from Geotail, proved strong onset related activity in the middle tail, roughly at distances of 20–30 R_E [e.g., *Angelopoulos et al.*, 1992; *Nagai et al.*, 1998; *Baumjohann et al.*, 1999; *Miyashita et al.*, 2000; *Nakamura et al.*, 2001a, 2001b]. The most pronounced signatures of this activity, such as bursty bulk flows [*Angelopolous et al.*, 1994] and plasmoids [*Ieda et al.*, 1998, 2001], are consistent with the near-Earth neutral line (NENL) model recently reviewed by

Baker et al. [1999]. This model was strongly supported by observations of extremely stretched and narrow plasma sheet prior to onset [*Sergeev et al.*, 1990, 1995; *Pulkkinen et al.*, 1999] and statistical analysis of plasma flows measured by AMPTE/IRM in the near-Earth environment during onsets [*Shiokawa et al.*, 1998]. Noting that the main postulates of the NENL model from the initial reconnection onset to the substorm current wedge launch and recovery were confirmed by simulations [*Birn and Hesse*, 1996; *Birn et al.*, 1999], the substorm problem would have been resolved if it had not met substantial problems in explaining near-Earth processes and dynamics of preonset arcs and pseudo-breakups reviewed above. A physically robust idea of flow braking at $\geq$10 R_E as a possible way to explain processes observed in the near-geostationary regions and at the equatorward edge of the auroral oval [*Haerendel*, 1992; *Shiokawa et al.*, 1997, 1998] apparently faces some quantitative limitations in producing impulsive near-Earth breakup and long lasting substorm current wedges of large amplitudes. Stronger effects may potentially be provided by the magnetic field and pressure buildup [*Birn and Hesse*, 1996] but this mechanism appears to be complementary to the ever present pressure gradients at the inner edge of the plasma sheet. These points bring energy sources and possible instabilities at the inner edge of the plasma sheet back to the stage.

[11] *Liou et al.* [1999, 2000] compared different signatures of onset and concluded that the most robust timing indicator is breakup brightening that typically overtakes other signatures of the expansive phase commencement. Therefore, an essential step toward a comprehensive substorm concept is comparison of auroral signatures with plasma sheet dynamics. In the last few years, extensive studies were undertaken in order to identify an auroral breakup, or brightening, using Polar imagers with respect to magnetotail dynamics observed by Geotail [*Fairfield et al.*, 1999; *Ohtani et al.*, 1999; *Pulkkinen et al.*, 1999; *Yahnin*, 2000; *Nakamura et al.*, 2001a, 2001b; *Frank et al.*, 2001a, 2001b; *Ieda et al.*, 2001]. The obtained results turned out to be controversial, supporting both near-geostationary and midtail origins [e.g., *Yahnin*, 2000]. This apparent contradiction might be caused by insufficient midtail observation points and fast variations of the plasma sheet parameters. However, in our opinion, this controversy is mainly a result of the limits of Polar optical instruments in detecting the true moment of breakup, due to restricted spatial resolution and line of sight integrated luminosity effects imposed on images. As seen from ground-based observations, the initial arc has a thickness on the order of tens of kilometers and it brightens for several minutes before a vortex forms and expands poleward [e.g., *Voronkov et al.*, 2000a, 2000b] (Lyons et al., manuscript submitted, 2002), a process which is traditionally called breakup. A breakup arc may stay very closely to preexisting growth phase arcs that obscure initial brightening (Lyons et al., manuscript submitted, 2002). As well, the initial brightness of vortices varies significantly (ten times or more) from one event to another [*Voronkov et al.*, 2000a]. As a result, it is not clear what stage of vortex development will be identified in the Polar data as "the breakup".

[12] This question emphasizes the significance of using high resolution ground-based optical observations in order to identify initial dynamics and timing of the auroral breakup for further comparison with the magnetosphere processes. Although this kind of study has a long history [e.g., *Koskinen et al.*, 1993; *Nakamura et al.*, 1994; *Petrukovich et al.*, 1998; *Aikio et al.*, 1999], now we have a new opportunity to revisit the problem using better ground based and in situ observations. Obviously, a good conjunction of several observational ground based and in situ sites is a rare occurrence. Hence, the recent progress have been achieved with "event studies" [e.g., *Petrukovich et al.*, 1998; *Aikio et al.*, 1999]. Our present work also is an event study with strategy similar to that used by *Koskinen et al.* [1993] and *Aikio et al.* [1999].

2. Instruments

[13] The main ground-based instrumental network used for this study is the Canadian Auroral Network for the OPEN Program Unified Study (CANOPUS) that consists of a magnetometer array, meridional scanning photometers (MSPs) at Rankin Inlet (RANK), Gillam (GILL), Pinawa (PINA), and Fort Smith (FSMI), and an All Sky Imager (ASI) at Gillam. The standard MSP data set has one minute resolution with 17 bins in the meridional scan. Higher resolution MSP data from Gillam, with 80 bins sampled every 30 s, is also used in this paper. The Gillam ASI frame rate is one per minute for both 557.7 and 630 nm. A more detailed description of the CANOPUS instruments can be found in the studies by *Rostoker et al.* [1995], *Voronkov et al.* [1999], and *Samson et al.* [2000, available at http://dan.sp-agency.ca/www/sub_info. htm].

[14] Our study focuses on optical data from CANOPUS instruments on the Churchill meridian. It is crucial, therefore, that we have magnetometer coverage both East and West of the Churchill line. The latter is taken care of by the CANOPUS magnetometers (i.e., Rabbit Lake, etc.). For coverage East of Churchill, we appeal to the Natural Resources of Canada (NRCan) magnetometers located at Poste-de-la-Balein (PBQ) and Ottawa (OTT). All magnetic data have 5 s resolution. We also used the poleward stations of the IMAGE magnetometer array (Ny Ålesund, Longyearbyen, Hornsund, Hopen Island, and Bear Island) along with the CANOPUS Taloyoak (TALO) to monitor high-latitude magnetic activity to provide a proxy of global magnetospheric convection.

[15] In this study, we used one minute Wind solar wind parameters, standard (1 min) and high resolution (0.5 s) magnetic data from the GOES 8 and GOES 9 geostationary satellites that were in the evening and premidnight sectors, respectively, bracketing the CANOPUS Churchill line, and Geotail standard and high resolution data of magnetic and electric fields and plasma parameters (see *J. Geomagn. Geoelectr.*, *46*, 1994, the CDAWeb page at http://cdaweb.gsfc.nasa.gov/cdaweb/, and the Darts-Geotail web page at http://www.darts.isas.ac.jp/spdb/index.html for details). As mentioned above, Geotail was near the equatorial plane in the midnight sector at $\sim$19 R_E down the tail. As mentioned in section 1, Figure 1 is a map of ground-based sites (except the IMAGE magnetometers), positions of the geostationary satellites GOES 8 and GOES 9 and the trajectory of Geotail for 0400–0800 UT mapped using the Tsyganenko 89 model [*Tsyganenko*, 1989]. The grid in Figure 1 corresponds to the

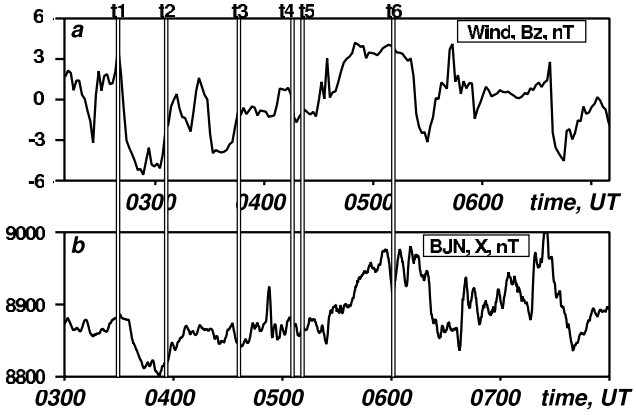

Figure 2. Solar wind B_z by Wind (a) and the magnetic X-component by the IMAGE Bear Island magnetometer (b). Vertical bars indicate the beginning of the growth phase (t1); start of pseudo-breakup further developed into a local substorm (t2); recovery of the local substorm and the beginning of the second growth phase (t3); breakup (t4); full substorm onset (t5); poleward boundary intensification at the substorm recovery phase (t6).

PACE Geomagnetic coordinate system [*Baker and Wing*, 1989].

3. 19 February 1996 Event Summary

[16] Data (for the entire sequence of events) is presented in Figures 2–4 illustrating the solar wind B_z magnetic field component, high latitude magnetic field variations, and the most distinct features seen by the CANOPUS and in situ instruments. All data presented in these plots is of a "standard" format available from the Internet CDAWeb and DARTS-Geotail websites, and from the CANOPUS database (Canadian Space Agency). Vertical bars show commencement of the main processes that are discussed in more detail in sections 4–9. Timing (except for the Wind data) for the vertical bars are as follows: t1 = 0330 UT—beginning of the growth phase; t2 = 0352 UT—start of pseudo-breakup further developed into a local substorm; t3 = 0435 UT—recovery of the local substorm and start of the second growth phase; t4 = 0506 UT—breakup; t5 = 0510 UT—full substorm onset; t6 = 0601 UT—start of the poleward boundary intensification. t1 was defined as the first signature of convection enhancement registered by the TALO magnetometer as described in section 4. For t2–t6 we used auroral signatures according to the CANOPUS optical data (see sections 5–8 for details).

[17] Magnetic field variations from the Wind satellite (B_z component) and the corresponding magnetic field response observed in the polar cap region (Bear Island X-component) are shown in Figures 2a and 2b, respectively. Estimated time for the solar wind features to reach the magnetopause was 50 min.

[18] Merged photometer data from Gillam and Rankin Inlet MSP are plotted in Figures 3a–3c and show the intensity of 486.1-, 557.7-, and 630.0-nm emissions, respectively. Magnetic X-component data from the Churchill line magnetometers are combined in Figure 3d.

[19] Selected satellite data is summarized in Figure 4: magnetic field components (in Local Spacecraft Coordinates) from GOES 8 H_p, directed perpendicular to the orbit plane, and H_n, directed eastward, (Figures 4a and 4b, respectively), H_p component from GOES 9 (Figure 4c), and B_z, B_x (both in the GSE coordinates), duskward component of the electric field, Earthward flow (V_x in the GSE coordinates), and average ion energy from Geotail (Figures 4d through 4h, respectively).

4. Growth Phase

[20] Except for two short-term pulses in the IMF, the solar wind was steady and quiet with northward magnetic field before ~0240 UT, as indicated by the Wind measurements in Figure 2a. At 0244 UT, Wind registered a southward IMF reversal that reached its minimum at 0253 UT and lasted for roughly 15 min. Taking the spacecraft position (174, 14.5, 12) R_E, the solar wind velocity ~470 km/s, and assuming the magnetopause to be at 12 R_E, we can expect the beginning of the growth phase at roughly 0330–0340 UT. This start of the growth phase was quite clearly observed at 0330–0335 UT by different instruments. The pulse of convection enhancement was registered by the TALO magnetometer at 0330 UT (t1 in Figures 2–4) and at 0335 UT by the IMAGE high latitude magnetometers. The CANOPUS photometer at Gillam demonstrated equatorward motion of the proton aurora band that started at 0337 UT (Figure 3a) which is consistent with a time delay between growth phase signatures on closed and open field lines [*Voronkov et al.*, 1999].

[21] Geotail registered a pulse of duskward electric field and Earthward flow after 0332 UT (Figures 4f and 4g). This pulse appeared on the background of a decreased plasma pressure (from 1.2 to 0.4 nPa) after which it increased to 2 nPa and remained at that level almost until breakup (t4 in Figures 2–4). This suggests that at the time of the growth phase commencement, Geotail was outside the plasma sheet and the electric field pulse could have been of both temporal and spatial character. After 0340 UT, the central plasma sheet expanded over Geotail, and the spacecraft remained in the central plasma sheet for the rest of the growth phase and during the whole pseudo-breakup and local substorm, as suggested by the magnetic field (Figures 4d and 4e) and ion temperature (Figure 4h) measurements.

[22] GOES 8 was in the premidnight sector when the growth phase started. The H_p reduction was seen after 0332 UT when GOES 8 was at 2212 MLT, indicating energy storage in the near-geosynchronous region (Figure 4a).

5. Pseudo-Breakup and Local Substorm

[23] Pseudo-breakup at 0352 UT might have been triggered by a northward turning of the solar wind B_z which was registered by Wind (Figure 2a) and caused global convection decrease as suggested by the high latitude magnetic variations (e.g., Figure 2b). This pseudo-breakup was clearly observed close to the zenith of the Gillam ASI and the vortex dynamics of the whole pseudo-breakup were covered by the ASI field of view, as suggested by the multi-instrument observations discussed below. We illustrate the dynamics of pseudo-breakup and the following local substorm by combining different ground-based observations in

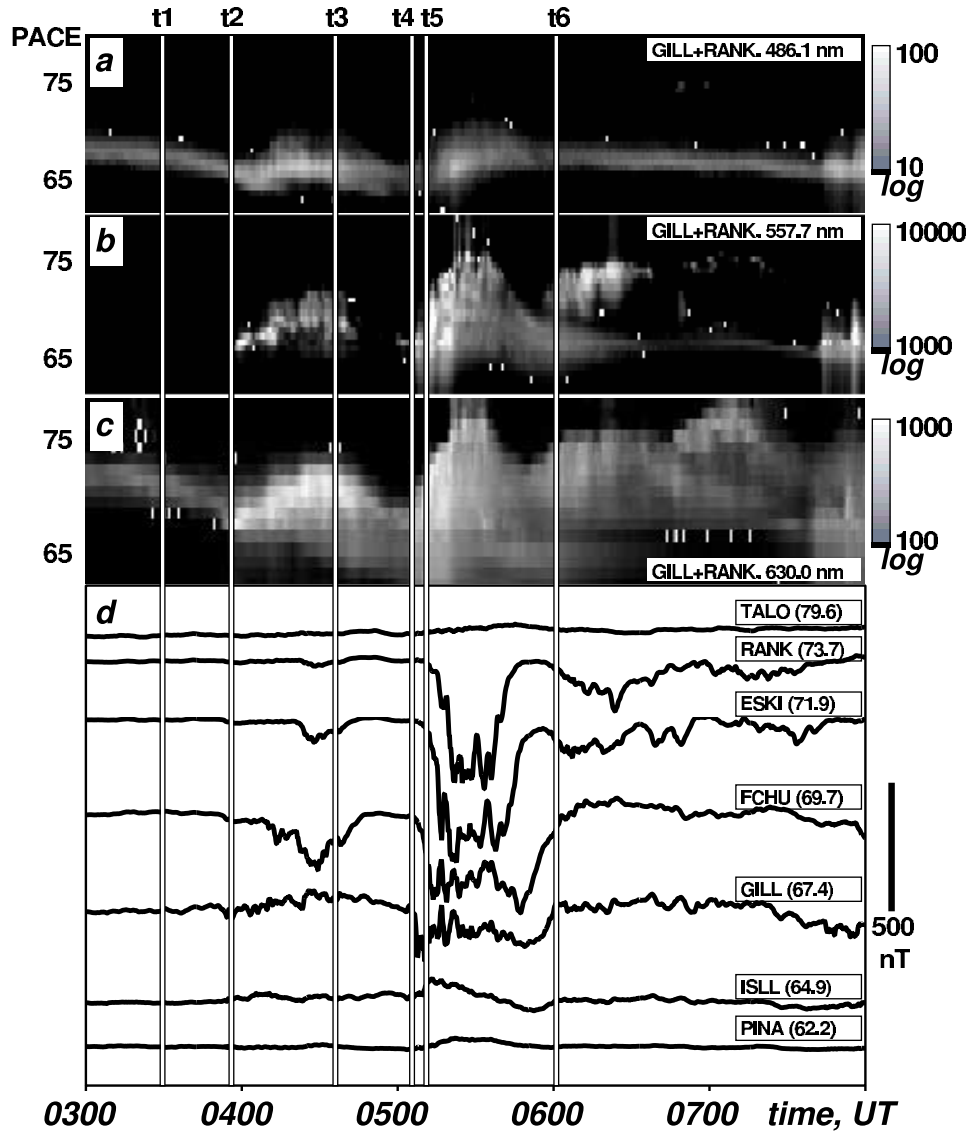

Figure 3. Summary plot of some ground based data for the whole event: merged GILL and RANK MSP data for 486.1 nm (a), 557.7 nm (b), and 630.0 nm (c) emissions, and *X*-component of the magnetic field at the Churchill line (d). PACE latitudes of the Churchill line magnetometers are shown in brackets. Notations for the vertical bars are the same as in Figure 2.

Figure 5. The 630.0 nm ASI images are mapped assuming that the emission altitude was 230 km and overlaid with bars indicating the position and width of the proton aurora band (westward and more equatorward bar aligned with the Gillam MSP scan) and the electron precipitation region (eastward and more poleward bar aligned with the Rankin Inlet MSP scan). In order to estimate the latitudinal extent of the proton and electron precipitation regions, we used 486.1 nm and 630.0 nm emission data, respectively, from the Gillam and Rankin Inlet MSPs. Altitudes for the emission origins were assumed as 110 km for the 486.1 nm emission and 230 km for the 630.0 nm emission. The widths of both regions were estimated as latitudinal ranges where the emissions were greater than I_{max}/e, where I_{max} is the maximum intensity at this time. This approximation corresponds to interpolation of both regions as Gaussian profiles in the scan-aligned direction [*Friedrich et al.*, 2001a, 2001b]. Vectors show deviation of the horizontal component of the magnetic field from the baselines computed as average values for two hours preceding the beginning of the growth phase, namely for 0130–0330 UT. Magnitudes of the magnetic perturbations are scaled as 20 nT per 1°.

[24] The equatorward arc intensified at 0352 UT (t2 in Figures 2–4) near the poleward boundary of the proton aurora band and the equatorward boundary of the diffuse electron precipitation region (Figure 5a). The maximum intensity of the arc was observed at 67.6° PACE latitude which was 0.5° poleward of the latitude of the peak proton aurora intensity. The arc manifested a large arc-aligned perturbation characterized by the ratio $k\delta$ on the order of 0.7, where k is the arc aligned wave number and δ is the half thickness of the arc, which is a characteristic initial perturbation for breakups [*Voronkov et al.*, 2000a]. This initial perturbation developed into the pseudo-breakup vortical structure that expanded

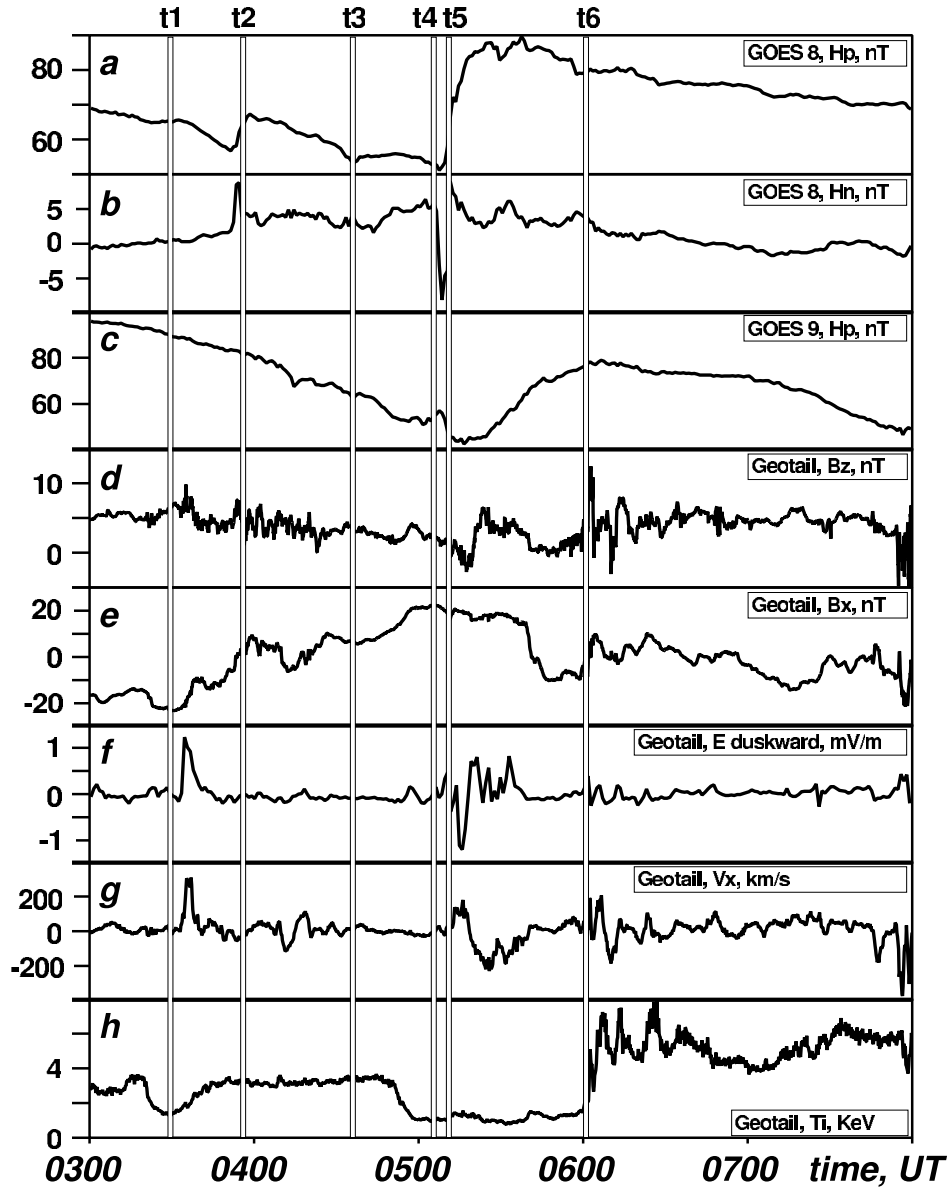

Figure 4. Summary plot of some satellite data for the whole event: H_p component of the magnetic field by GOES 8 (a), H_n component of the magnetic field by GOES 8 (b), H_p component of the magnetic field by GOES 9 (c), and Geotail data for the B_z component of the magnetic field (d), B_x component of the magnetic field (e), duskward component of the electric field (f), V_x component of the bulk velocity (g), and average energy of ions (h). Notations for the vertical bars are the same as in Figure 2.

poleward (Figure 5b for the 0356 UT image). By roughly 0400 UT, growth saturated when the vortex was still near the proton aurora poleward boundary. This was the end of optical pseudo-breakup. However, the magnetic perturbations were still growing at this stage. Magnetic vectors shown in Figures 5c–5e suggest that a near-azimuthal electrojet system forming the local substorm equivalent current structure was growing in the vicinity of the auroral vortex up to roughly 0430 UT, followed by a decrease in current.

[25] In the longitudinal direction westward of Gillam, magnetic signatures of the local substorm expansion were seen only in Rabbit Lake at ~0410 UT, roughly at the westward edge of the vortex as seen in Figure 5d. No other ground based instruments westward of Rabbit Lake registered noticeable signatures. These observations are consistent with the magnetic field data from GOES 9 (Figure 4c). Combination of the ground-based and GOES 9 signatures indicates that the westward extension of the whole process did not propagate much westward from the ASI field of view.

[26] Figure 6 shows the dynamics of pseudo-breakup as seen using the high resolution GOES 8 magnetic data (Figure 6a for the H_p component) and high resolution Gillam MSP data of the 630.0-nm emission (Figure 6b). Dynamics of the prebreakup arc at the equatorward edge of the electron precipitation region is highlighted in Figure 6c, and the magnitude of the arc brightness is shown in Figure 6d. The initial arc intensification fits the dependence of the form $I = I_0 \exp^{\gamma t}$ with the growth rate $\gamma = 0.012\ s^{-1}$. This

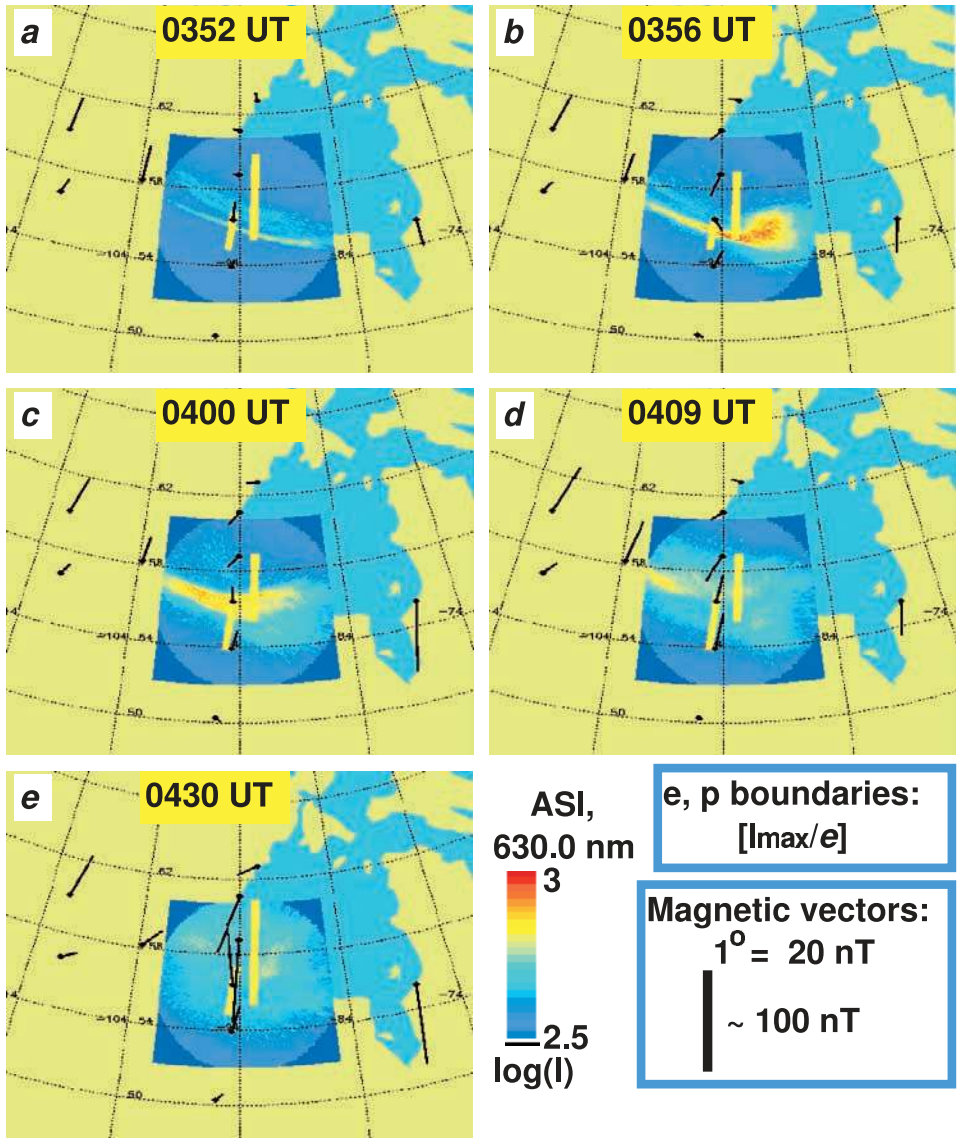

Figure 5. Overlays of ground based optical and magnetic observations for the main stages of the pseudo-breakup: initial arc (0352 UT), vortex formation (0356 UT), vortex saturation (0400 UT) and dissipation (0409 and 0430 UT). Arrows indicate horizontal magnetic perturbation vectors scaled as 20 nT per 1°, and bars show the widths of the proton aurora region (westward and more equatorward bar aligned with the Gillam MSP scan) and the electron aurora region (eastward and more poleward bar aligned with the Rankin Inlet MSP scan). Grid is geographic.

growth corresponded to the final prebreakup decrease in the magnetic H_p component at the GOES 8 position. Vortex formation led to increased brightness but the growth rate was reduced compared to the initial intensification. This vortex formation and its poleward expansion matched the beginning of the dipolarization at the geostationary orbit, and abrupt onset of the high-frequency magnetic pulsations. Vortex saturation after 0357 UT corresponded to the end of dipolarization, according to GOES 8 data.

[27] It is possibly not a surprise that pseudo-breakup launched a wide spectrum of pulsations. The most distinct were high frequency (~45 mHz) and large amplitude (~30 nT) Pi1 pulsations seen by GOES 8, ~18 mHz Pi2 pulsations registered by GOES 8 and on the ground in the vicinity of the arc, and more global Pc5 waves in the range of 3–8 mHz. Figure 7 provides a quick-look diagram at timing and sequence of these pulsations as measured by the GOES 8 and Pinawa magnetometers.

[28] Near the end of the initial growth of arc brightness leading to the vortex expansion at 0352–0353, explosive onset of Pi1 pulsations was registered by GOES 8 (see Figures 6a and 7a). Despite the very large amplitude of these waves, they were seen only by GOES 8 and for a short time during the vortex expansion stage. The spectrum of these pulsations had a broad distribution centered around 46 mHz, as shown in Figure 8. The explosive onset, broad spectrum, spatially local character, and rapid damping (perhaps explaining the absence of these pulsations on the ground) imply that these waves were of dispersive and probably turbulent nature.

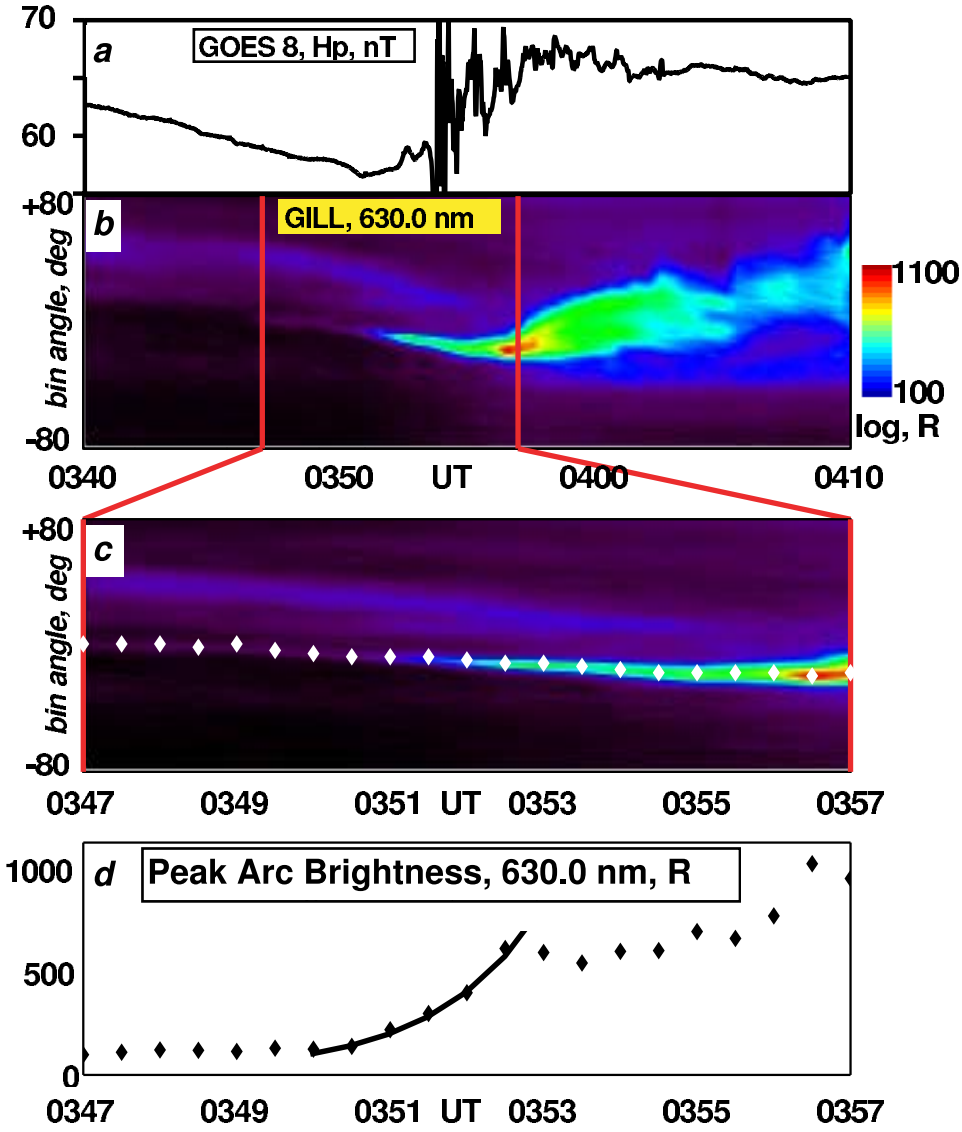

Figure 6. Comparison of high resolution GOES 8 and Gillam MSP data: H_p component of the magnetic field by GOES 8 (a), 630 nm emission by the Gillam MSP (b) with highlighted interval (c) in which diamonds point the position of the arc brightness maxima, and the magnitude of the arc brightness for the highlighted interval (d). In (d), the arc intensification is compared with the function $I = I_0 \exp^{\gamma t}$ with the growth rate $\gamma = 0.012$ s^{-1}, shown as a solid line.

[29] Pi2 pulsations at ~18 mHz were registered almost simultaneously at 0352–0400 UT by all CANOPUS magnetometers in the vicinity of the arc (e.g., Figure 7b for Pinawa), by GOES 8 (Figures 6a and 7a), and by Geotail. However, they were not seen in longitudinal sectors westward of the arc. This suggests that the arc current system might be the origin of these pulsations. This conjecture is also supported by the latitudinal Pi2 amplitude distribution shown in Figure 9. The Pi2 pulsation spectrum observed by GOES 8 is compared to the spectrum obtained using Pinawa data in Figure 8. The similarity of these spectra in the Pi2 range suggests that GOES 8 was on subauroral field lines and Earthward of the magnetospheric origin of this pseudo-breakup. Some other features such as the dispersive character of the Pi1 waves, the simultaneous enhancement of Pi2s at GOES 8 and Geotail, and the periods of Pc5 pulsations discussed below, also support the idea that this pseudo-breakup originated tailward of geostationary orbit.

[30] Enhancement of Pc5 pulsations with frequencies of 3–8 mHz (depending on latitudes) was first registered by magnetometers near the auroral arc, GOES 8, and Geotail after ~0352 UT, matching the very beginning of the pseudo-breakup vortex formation. However, after 0400 UT, these pulsations were seen globally by all the CANOPUS magnetometers and GOES 9 in the evening sector. In Figure 10 we compare the latitudinal profiles of Pc5 amplitudes with the 630 nm intensity profile obtained by the GILL and RANK MSPs. Both profiles represent average values for the time interval of 0400–0430 UT. The similarity of these profiles suggests that the Pc5 pulsations were closely connected with the region of the optical pseudo-breakup and following local substorm. On the other hand,

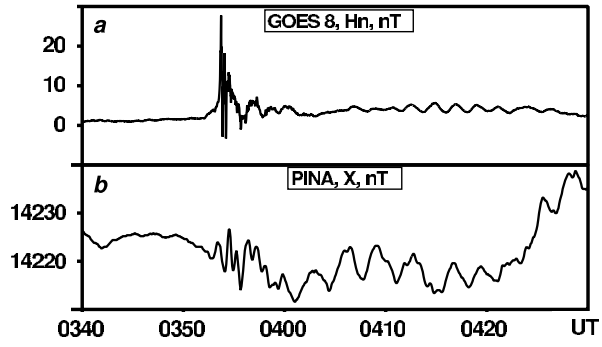

Figure 7. H_n component of the magnetic field by GOES 8 during pseudo-breakup (a) compared to the X component of the magnetic field in Pinawa (b).

the latitudinal dependence of the Pc5 frequencies allows an approximate mapping of the pseudo-breakup region with respect to the GOES 8 and Geotail positions. The Pc5 spectrum observed by Geotail is close to that obtained using Fort Churchill magnetic data (Figure 11a), indicating that Geotail was tailward of the region of the pseudo-breakup. At the same time, comparison of near-monochromatic waves observed by GOES 8 after pseudo-breakup (Figure 7a) with those from ground-based observatories showed a close agreement of the ~8 mHz peak seen by GOES 8 with corresponding pulsations in Ottawa (Figure 11b). This indicates that after pseudo-breakup, GOES 8 ended up at midlatitude field lines, mapping even further equatorward from the vortex position than it was during pseudo-breakup. Overall, analysis of Pc5 spectra suggests that the whole pseudo-breakup and local substorm process was confined in the region tailward of geostationary orbit but Earthward of the Geotail position at 19 R_E.

6. Second Growth Phase

[31] After pseudo-breakup, the second growth phase with classical signatures, and similar in character to the first growth phase, was seen after roughly 0435 UT (t3 in Figures 2–4) by ground-based and spacecraft instruments.

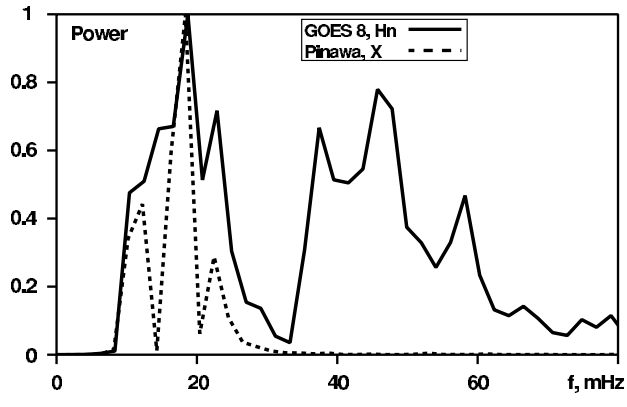

Figure 8. Power spectra in normalized arbitrary units of high frequency pulsations in the H_n component seen by GOES 8 (solid line) and X component in Pinawa (dashed line) for the 0352–0400 UT interval.

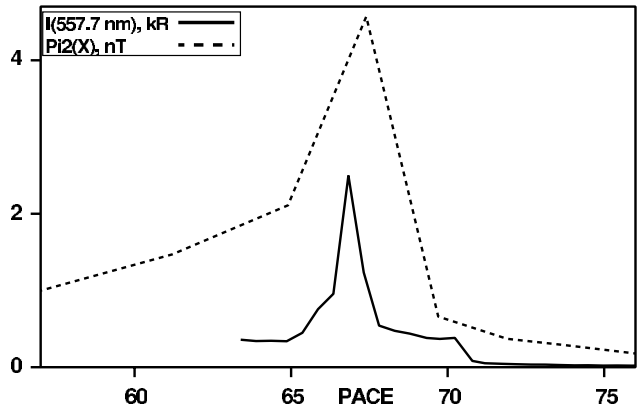

Figure 9. Latitudinal profiles of arc intensity in the 557.7 nm emission line at 0356 (solid line), and Pi2 amplitudes (dashed line) averaged over 0354–0358 UT interval.

However, there was a quite important feature that distinguished the second growth phase from the growth phase preceding the pseudo-breakup. This period of time was characterized by the gradual dimming and narrowing of the electron aurora zone seen by the Gillam MSP (Figure 12a) and thinning of the plasma sheet as suggested by magnetic field variation registered by Geotail (Figure 12b). By the end of this growth phase, 630 nm emissions were at airglow level. This decrease in emission intensities, or aurora dimming effect, has been repeatedly observed during the late growth phase [*Pellinen and Heikkila*, 1978]. This interval corresponded to the maximum stretching of the tail: B_x became roughly 5 times greater than B_z at Geotail. In Figure 12c, we show the maximum intensity of the 630.0 nm emission as a function of the magnetic inclination seen by Geotail. This apparently new quantitative relation between emission intensities and magnetic field inclination in the magnetotail requires more statistical study but for this case, it is suggestive of a physical dependence.

7. Breakup and Substorm Onset

[32] Figure 13 is a summary plot for the substorm expansive phase following the growth phase discussed in

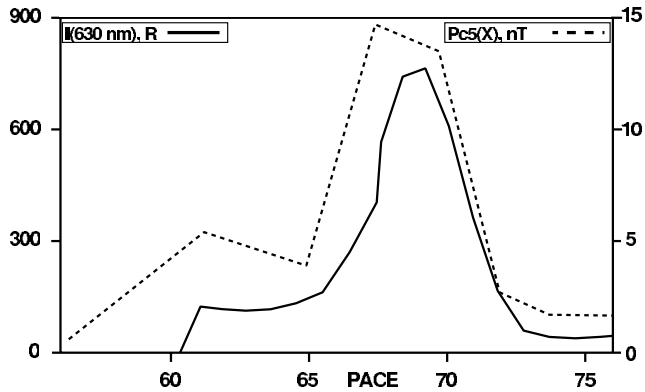

Figure 10. Latitudinal profiles of 630 nm emission (solid line) and Pc5 amplitudes (dashed line), averaged over 0400–0430 UT interval.

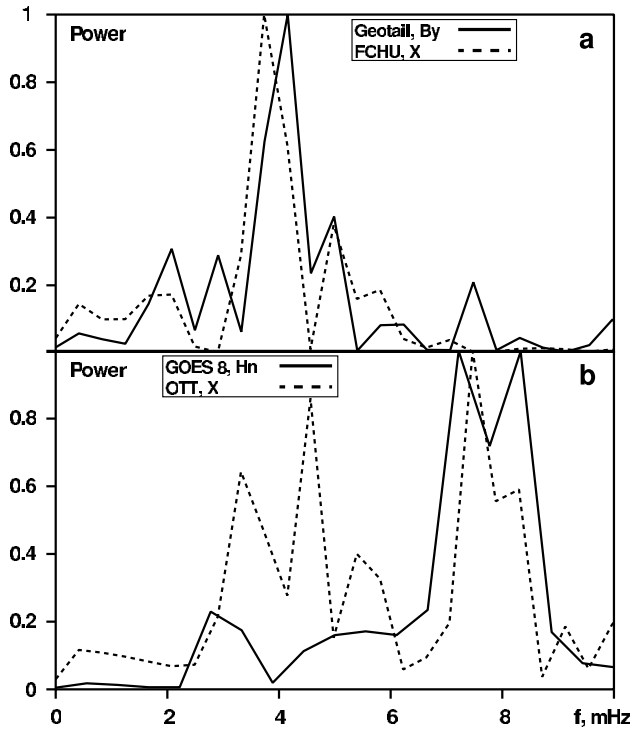

Figure 11. Power spectra in normalized arbitrary units of post-pseudo-breakup Pc5 pulsations: in the B_y component seen by Geotail (solid line) and in X component at Fort Churchill (dashed line) (a), and in the H_n component seen by GOES 8 (solid line) and in X component at Ottawa (dashed line) (b), for the 0400–0430 UT interval.

the previous section. This summary plot overlaps with Figures 3 and 4 but shows more details specific to the substorm onset and expansive phase.

[33] Substorm onset consisted of three distinct parts. The first two processes, arc intensification and breakup, were similar in character as for the pseudo-breakup described in section 5. These processes started at times shown in Figure 13 as vertical bars ts1 = 0459 UT and ts2 = 0506 UT (which is t4 in Figures 2–4), respectively. Full onset of the expansive phase started at time ts3 = 0510 UT (t5 in Figures 2–4) following breakup. Let us consider signatures of these three parts in more details.

[34] As shown in the previous section, the growth phase ended up with extreme thinning of the plasma sheet corresponding to a latitudinal narrowing of the electron precipitation region and a dimming of the diffuse aurora. At 0451 UT, the IMAGE magnetometer data showed significant changes in global convection (Figure 2b). After 0451 UT, Geotail registered growing low frequency pulsations in the dawn-dusk component of the electric field (Figure 13g). These pulsations reached a large amplitude, on the order of 1 mV/m, during the expansive phase and vanished after ~0520 UT at the beginning of the substorm recovery phase. We note that these pulsations were not accompanied by significant variations in the main magnetic field topology at the Geotail site until full onset of the expansive phase at 0510 UT (Figure 13f).

[35] Commencement of the cross-tail electric field pulsations was followed by intensification of a discrete arc at the poleward edge of the proton aurora as shown in Figure 14a. This intensification was also registered by the Gillam MSP after 0459 UT (Figure 13c). Similar to the pseudo-breakup case, arc brightening was rather slow. At geostationary orbit, this growth corresponded to the final reduction of the H_p component (Figure 13e) preceding dipolarization.

[36] The second stage, namely breakup at the time ts2 in Figure 13, was characterized by poleward expansion of auroras from the position of the initial arc as illustrated by the 0507 UT image in Figure 14b. Optical breakup corresponded to the explosive commencement of short period pulsations seen by GOES 8 as shown in Figure 15 which provides further evidence that this breakup was similar to the pseudo-breakup described in section 5. Namely, the initial arc intensification corresponded to the late growth phase whereas the optical breakup was seen almost simultaneously with the explosive onset of short period pulsations and the beginning of dipolarization at the geostationary orbit. After the first explosive burst, these pulsations vanished. However, different than the pseudo-breakup, this first package of pulsations was followed by the second burst of short period pulsations

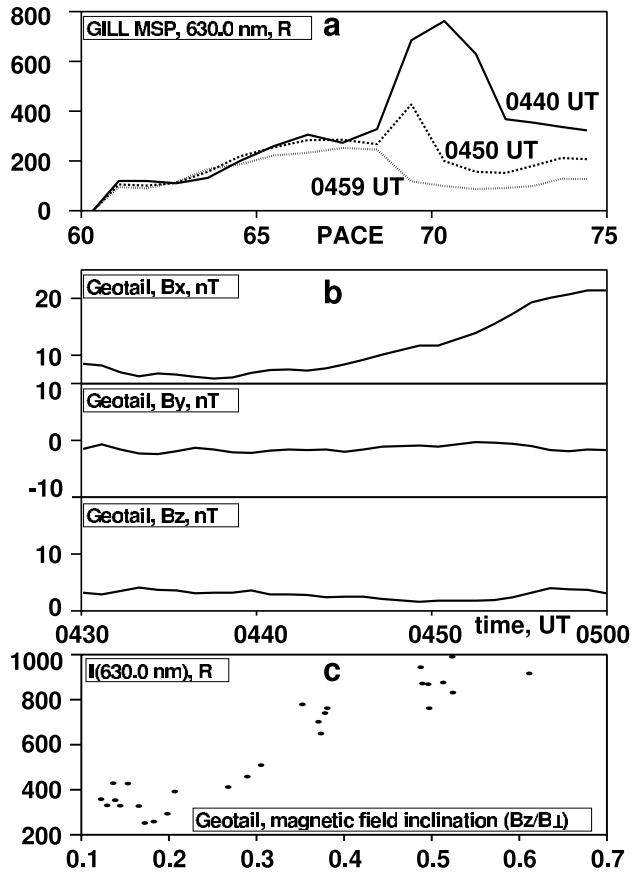

Figure 12. Latitudinal profiles of electron precipitation zone as seen by the Gillam MSP in the 630 nm emission line at 0440 UT (solid line), 0450 UT (dashed line), and 0459 UT (dotted line) (a), time evolution of the magnetic field components at the Geotail site (b), and dependence of the maximum intensity of 630 nm emission by Gillam from the magnetic inclination at the Geotail position (c).

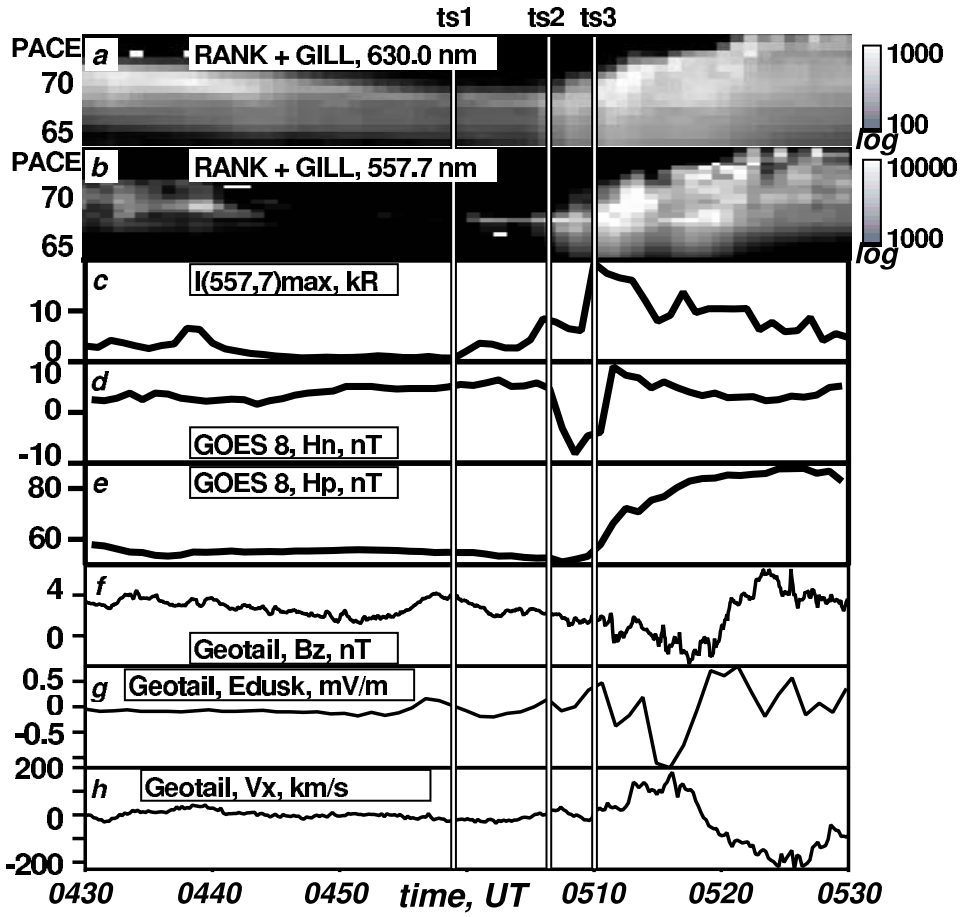

Figure 13. Temporal evolution of merged GILL and RANK MSPs 630.0 nm (a) and 557.7 nm (b) emissions, maximum intensity of the 557.7 nm emission (c), GOES 8 H_n (d) and H_p (e) magnetic component, and Geotail B_z (f), E_{dusk} (g), and V_x (h) during the substorm. Vertical bars indicate time of initial arc intensification (ts1), breakup (ts2), and full substorm onset (ts3).

most likely associated with the expansive phase onset (ts3). These pulsations were significantly larger in amplitude, and longer lasting, than those during breakup, possibly indicating larger energy input in the inner magnetosphere.

[37] Amplitudes of Pi2 pulsations with a period of ~1 minute observed by the Gillam, Rankin Inlet, and Geotail magnetometers are plotted in Figure 16. On the ground, the first package of Pi2 was seen locally near the arc at the time of breakup after 0505 UT, as illustrated by Figure 16a.

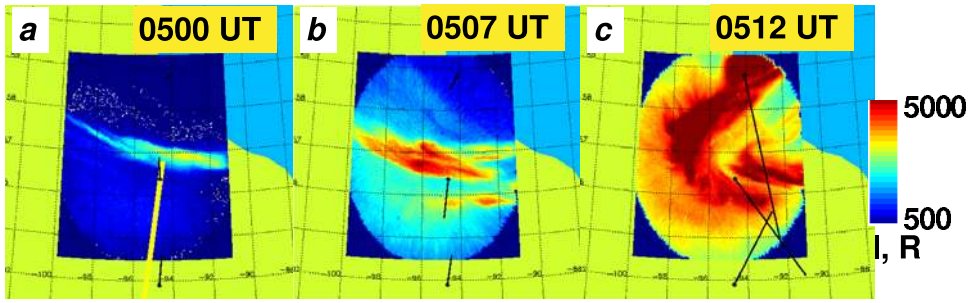

Figure 14. Overlays of ground based optical and magnetic observations for the main stages of breakup and full onset: an initial arc (0500 UT), breakup (0507 UT), and full onset surge (0512 UT). Arrows indicate magnetic perturbation vectors scaled as 50 nT per 1°. The yellow bar in (a) shows the width of the proton aurora region. Grid is geographic.

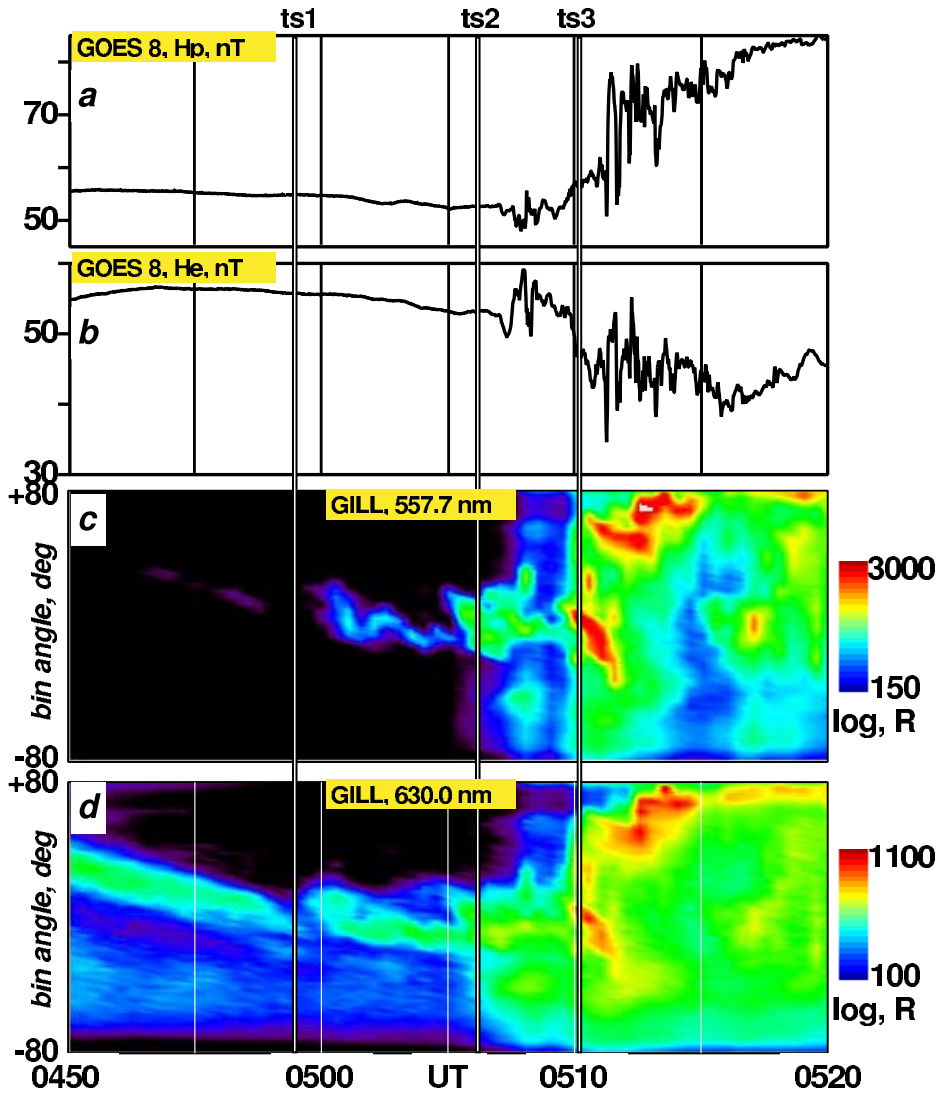

Figure 15. Comparison of high resolution GOES 8 and Gillam MSP data: H_p (a) and H_e (b) components of the magnetic field by GOES 8, and 557.7 (c) and 630 (d) nm emissions by the Gillam MSP. Vertical bars indicate time of initial arc intensification (ts1), breakup (ts2), and full substorm onset (ts3).

The second and more prominent period of Pi2 activity started at the expansive phase onset time (~0510 UT) and was seen globally. The commencement of this second Pi2 package was registered almost simultaneously, within 1–2 min by all auroral zone magnetometers in the Canadian sector, Geotail, and the geostationary satellites.

[38] Beyond the large amplitude Pi2s, the expansive phase onset at 0510 UT was characterized by other global processes in the near-midnight sector. The most pronounced signatures of this stage were as follows. MSPs observed fast poleward expansion of the energetic electron precipitation region starting at 0510 UT in different longitudinal sectors. At this time, the ASI image revealed a cell-like excursion of the poleward boundary of the electron precipitation region (Figure 14c), an optical signature that we suggest is associated with midtail reconnection [*Voronkov et al.*, 2000b]. This auroral cell corresponded to a strong curl of the magnetic field in the region. Finally after the expansive phase onset, Geotail registered significant disturbances at 19 R_E, such as strong pulses of cross-tail electric field, negative B_z followed by dipolarization, and the Earthward plasma flow.

[39] The expansive phase onset caused significant compression of the near-Earth magnetosphere. Thus the magnetic field at the geostationary orbit reached a magnitude of ~100 nT (Figures 4a and 13e) matching the order of magnitude of the dipolar magnetic field. Total dipolarization corresponded to the beginning of the substorm recovery phase characterized by magnetic field relaxation in the magnetotail accompanied by a tailward flow seen by Geotail after ~0515 UT (Figures 4d–4g and 13f–13h). After this time, the main auroral zone recovered to its predisturbed condition (e.g., Figure 3b). However,

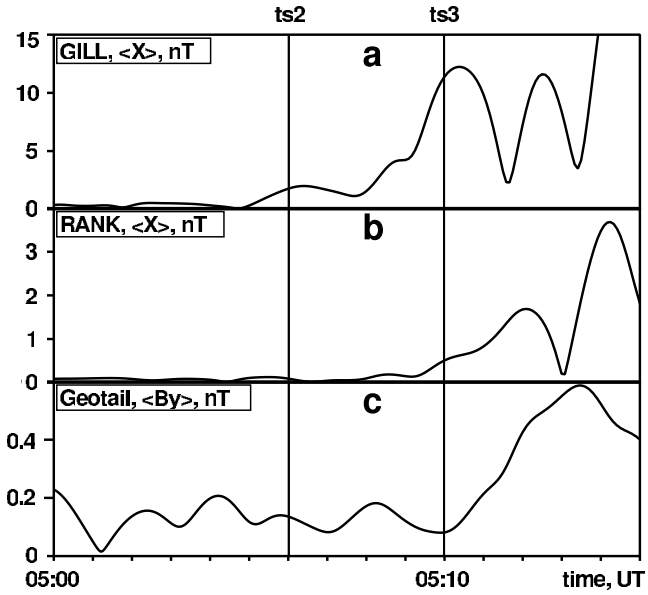

Figure 16. Amplitudes of the Pi2 pulsations in the range of 12–22 mHz seen by the Gillam (a), Rankin Inlet (b), and Geotail (c) magnetometers.

poleward of the main electron precipitation zone, the Rankin Inlet MSP registered prolonged pulses of electron precipitation apparently corresponding to the postsubstorm disturbances of the magnetotail. In the following section we deal with the dynamics of this poleward boundary intensification.

8. Poleward Boundary Intensification

[40] Beginning at ~0535 UT, the poleward boundary of discrete emissions moved equatorward, indicating a gradual return to a distribution of electron precipitation more characteristic for unperturbed conditions (Figure 3b). After ~0600 UT, the Churchill line MSPs registered the beginning of poleward boundary intensifications (PBIs). This new disturbance began at the poleward boundary of the receding electron precipitation region, at roughly 70° PACE latitude and propagated poleward to ~73° resulting in a clear separation of this precipitation region from the main auroral zone forming a double oval. This intensification was rather localized longitudinally for there were no clear optical signatures apparent in the Fort Smith MSP data.

[41] In Figure 17, we show the temporal evolution of the 557.7 emissions, as recorded by the Rankin Inlet MSP, and the midtail activity, as seen in the Geotail data. The sequence of PBIs after 0600 UT is clearly evident in the keogram (Figure 17a) and as a temporally structured increase in the peak brightness of the 557.7 nm emissions (Figure 17b). Geotail registered a bursty flow (Figure 17d) characterized by a sharp discontinuity in the magnetic field (Figure 17c) that also began at ~0600 UT. Enhancements in the ion temperature (Figure 17e) between 0600 and 0630 UT occurred at essentially the same time as enhancements

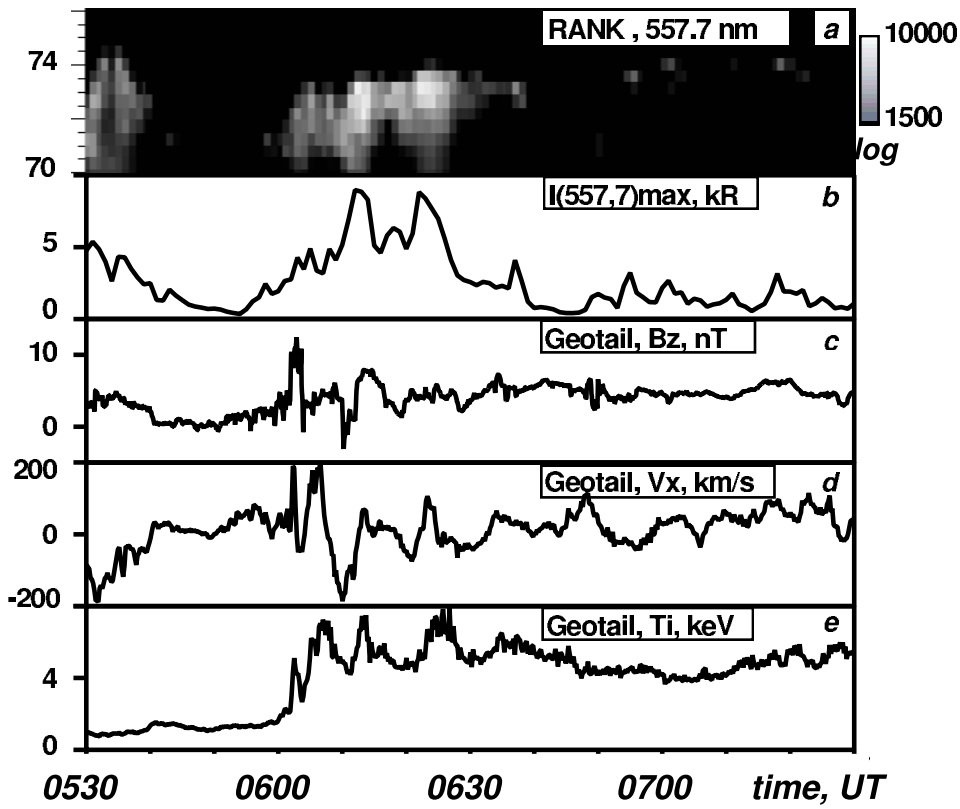

Figure 17. Temporal dynamics of the 557.7 nm emission measured by the Rankin Inlet MSP (a), maximum intensity of the 557.7 nm emission (b), and Geotail B_z (c), V_x (d), and T_i (e) during the poleward boundary intensification period at the substorm recovery phase.

in the 557.7 emissions and had a periodicity similar to the 557.7 nm emission pulses.

9. Discussion

[42] We have presented observations gathered during a period of magnetospheric activity that occurred on 19 February 1996. The sequence of events of interest was an initial growth phase, followed by a pseudo-breakup and local substorm, a second growth phase which began at the end of the local substorm and resulted in a breakup, full onset of the expansive phase, and a recovery phase. During the recovery phase, there was a double oval with embedded poleward boundary intensifications. This event was comprised of a clear sequence of substorm phases, and was free of prior activity. Careful analysis of observational data from such sequences of events [e.g., *Koskinen et al.*, 1993; *Nakamura et al.*, 1994; *Petrukovich et al.*, 1998; *Ohtani et al.*, 1999; *Pulkkinen et al.*, 1999; *Voronkov et al.*, 1999; *Aikio et al.*, 1999] are enormously valuable in terms of developing solid constraints of substorm theories and clarifying important questions concerning the magnetosphere-ionosphere mapping.

[43] More specifically, our goal has been to identify the ionospheric signature of midtail dynamics and the magnetospheric region magnetically conjugate to the breakup. We do not expect that this sequence of events is representative of all substorms. Nevertheless, we believe that a sequence of observed signatures will provide a useful framework for designing future multi-satellite and ground-based experiments affording greater temporal and spatial resolution. For this event study, we have presented data from a large number of ground-based instruments, as well as the GOES 8 and 9 geosynchronous satellites and the Geotail spacecraft which was located in the midtail region. In this section, we discuss these observations in the context of some recent relevant substorm works.

[44] The event began with a classic growth phase [*McPherron*, 1970], initiated by the southward turning of the IMF, and characterized by a marked enhancement of convection in the polar cap and the magnetotail (t1 in Figures 2–4). The beginning of this growth phase was clearly evident in the Geotail data. These Geotail signatures shown in Figure 4f–4g include a pulse of dawn-to-dusk electric field and corresponding enhanced Earthward convection. The inner magnetosphere growth phase signatures, such as magnetic field stretching, were clearly evident in GOES 8 magnetic field data indicating noticeable energy storage in the near-Earth plasma sheet.

[45] This growth phase resulted in a pseudo-breakup followed by a local substorm. This perturbation corresponded to a northward turning of the IMF and convection reduction in the polar cap suggesting that it was an externally triggered breakup [*Lyons*, 1995]. In fact, this event was included in the statistical study of substorm triggering carried out by *Lyons et al.* [1997].

[46] The pseudo-breakup was marked by an arc that brightened at the equatorward boundary of the diffuse electron aurora, and that developed a vortex structure. The arc and vortex were completely within the Gillam ASI field of view. ASI and high resolution photometer data revealed two distinct stages of the process: slow near-exponential arc intensity growth and breakup seen as vortex formation and its poleward expansion. Comparing optical signatures with magnetic field variation at the GOES 8 site, we note that the first stage corresponded to the final decrease of the H_p magnetic component at geostationary orbit. This stage of the growth phase was identified by *Ohtani et al.* [1992] as an ''explosive growth stage'' because of comparatively fast, on the order of minutes, cross tail current enhancement. The second stage, vortex formation and its poleward expansion, coincided with the beginning of dipolarization and the explosive onset of Pi1 and Pi2 pulsations at geostationary orbit. Pi2 pulsations detected by the ground-based magnetometers were observed in the near breakup region suggesting that the breakup was the source for these pulsations. The current wedge forming the local substorm that followed the pseudo-breakup was initially also confined within the optical breakup region. This supports models in which the near-geostationary plasmasheet as the origin for (pseudo-)breakup [e.g., *Kaufmann*, 1987; *Lui*, 1991; *Roux et al.*, 1991; *Lyons*, 1995; *Samson*, 1994; *Maynard et al.*, 1996; *Samson et al.*, 1998; *Ohtani et al.*, 1999; *Erickson et al.*, 2000; *Friedrich et al.*, 2001a, 2001b] and is contrary to the NENL models that suggest that the near-Earth plasmasheet and corresponding equatorward part of the auroral region are perturbed by the Earthward expansion of a midtail instability [e.g., *Baker and McPherron*, 1990; *McPherron*, 1992; *Shiokawa et al.*, 1998; *Baker et al.*, 1999; *Baumjohann et al.*, 1999; *Birn et al.*, 1999]. The clear sequence of events around this pseudo-breakup indicates that a midtail instability is not essential to trigger processes associated with auroral (pseudo-)breakups.

[47] The pseudo-breakup initiated wide-spread near-monochromatic oscillations of the night side magnetosphere with frequencies in the Pc5 band. Comparison of Pc5 spectra indicated that the Geotail position mapped roughly at latitudes of Fort Churchill, that matched the poleward edge of the optical pseudo-breakup and local substorm. The Pc5 frequency at the GOES 8 position matched the main frequency in the Pc5 spectrum in Ottawa suggesting the during the local substorm, GOES 8 occurred at midlatitudes quite equatorward of the local substorm region. Therefore, magnetosphere to ionosphere mapping using Pc5 pulsations suggested that the pseudo-breakup and local substorm occurred tailward of geostationary orbit but Earthward of Geotail at 19 R_E.

[48] The local substorm was followed by a second growth phase. The main distinction of this growth phase from the initial one was significant stretching of the magnetospheric magnetic field, seen in GOES 8 and 9 and Geotail data. This thinning has been repeatedly observed in situ prior to large substorms [e.g., *Sergeev et al.*, 1990, 1995; *Pulkkinen et al.*, 1999] which supports the idea that a thin current sheet is essential for a magnetotail disruption leading to a full substorm onset. Concurrent fading of the diffuse electron precipitation prior to onset [e.g., *Pellinen and Heikkila*, 1978], evident in the 630 nm MSP data, was almost certainly associated with the thinning of the plasma sheet as suggested by a good correlation between variations of magnetic inclination at Geotail and peak values of the 630 nm intensity measured by the Gillam MSP (Figure 12c).

[49] Following the second growth phase, the three stage commencement of the substorm expansive phase was observed. The first two stages, slow arc intensification followed by auroral vortex poleward expansion, were similar in character to the equivalent stages of the pseudo-breakup. The third stage, namely the expansive phase onset, involved strong magnetotail perturbations in magnetic and electric fields and an Earthward plasma flow (seen by Geotail), explosive enhancement of auroral precipitation and of the westward electrojet poleward of the initial breakup region, the second large amplitude package of Pi2 pulsations, and final wrap up of the aurora into a cell-like (or surge) structure. Magnetic and optical signatures of this third stage were registered near simultaneously by all CANOPUS instruments, indicating the global character of the full onset of the expansive phase. These observations consistently support the midtail disruption, or NENL, processes as the main source for the large energy release at the full substorm onset and during the following expansive phase [e.g., *Baker et al.*, 1999; *Baumjohann et al.*, 1999; *Birn et al.*, 1999].

[50] An exact identification of the recovery phase commencement for the large substorm is a challenging task outside of the goal of this study. Roughly after 0520 UT, the end of dipolarization at the GOES 8 site (Figures 4a and 13e) and recovery of the magnetic and electric fields at the Geotail position were evident (Figures 4d and 4f and 13f and 13g). This corresponded to the beginning of the substorm aurora and electrojet intensity decay and equatorward retreat of the poleward boundary of the electron precipitation region, as seen in Figure 3. However, during the recovery phase, a series of PBIs started at the poleward boundary of the diffuse aurora (as seen in the 557.7 and 630 nm MSP data shown in Figures 3b and 3c). These PBIs expanded poleward, resulting in a distinct double oval auroral distribution. The lack of emission between the PBIs and the inner diffuse auroral oval indicates a different magnetospheric origin for these two regions. Long period oscillations of these PBIs closely correlated with a sequence of bursty flows and plasma energy pulses registered by Geotail.

10. Summary

[51] The sequence of auroral and magnetospheric events on 19 February 1996 presented in this paper consisted of an initial growth phase, pseudo-breakup and local substorm followed by a second growth phase, and breakup followed by a full substorm. During the recovery phase of the resulting substorm, there were a double auroral oval and PBIs. Important details that have been elucidated in this sequence of events are:

1. In the initial growth phase, stretching of the magnetic field lines was observed at geostationary orbit indicating energy storage in the inner plasma sheet.

2. The energy storage in the second growth phase, preceding full substorm onset, led to significant topological changes both at geostationary orbit and in the midtail region. Stretching in the midtail was found to be in close correlation with dimming of auroral luminosity.

3. The pseudo-breakup and breakup both occurred in two stages. The first was arc intensification corresponding to the late growth phase. The second was vortex formation and poleward expansion, observed near simultaneously with the onset of short period (Pi1 and Pi2) pulsations and the beginning of dipolarization at geostationary orbit. Pi1 onset was explosive but local and rapidly vanishing.

4. Pseudo-breakup and breakup Pi2 pulsations observed on the ground started and saturated along with the optical breakup vortex. Their amplitudes were peaked in the breakup region.

5. Pseudo-breakup launched near-monochromatic Pc5 pulsations that were observed by all CANOPUS and in situ instruments involved in this study. Comparison of Pc5 frequencies indicates that the pseudo-breakup and local substorm occurred tailward of geostationary orbit but Earthward of Geotail at $\sim$19 R_E.

6. The full substorm onset that followed the breakup produced the second package of Pi2 pulsations that were of larger amplitude than breakup pulsations.

7. The recovery phase poleward boundary intensifications correlated with midtail plasma dynamics, namely, with bursty flows and plasma energy pulses.

[52] Considering these results, and relevant studies reviewed in sections 1 and 9, we suggest the following constraints for different elements of substorm activity. During the growth phase, a significant amount of energy is stored in the near-Earth plasma sheet. This energy can be released as a near-Earth pseudo-breakup, or breakup, that is an instability of the inner plasma sheet. A (pseudo-)breakup consists of two distinct stages. The first is arc intensification at the poleward slope of the proton aurora band. The second stage is vortex formation and its spatial expansion. This corresponds to the explosive onset of short period pulsations on the ground and at geosynchronous orbit, and the beginning of dipolarization in the near-Earth plasma sheet. At the same time, full substorm onset requires noticeable thinning of the plasma sheet in the midtail region apparently leading to the NENL formation. On the empirical level, it is suggested that breakup is a localized physical process in the near-Earth plasma sheet. It has a lower threshold than midtail reconnection onset, or full substorm onset, but provides comparatively low and local energy unloading.

[53] This still highlights the problem of interaction of different processes in the inner and midtail plasma sheet during full substorms. However, addressing such questions requires further statistical studies using better ground-based and in situ spatial coverage of the night side magnetosphere. Clearly, more detailed studies of such events, utilizing our ever increasing ground- and space-based observing capabilities, are essential to closure on the substorm problem. At the same time, these studies will provide a feedback in the design of future multi-spacecraft magnetospheric missions.

[54] **Acknowledgments.** The CANOPUS array is a ground-based facility funded and operated by the Canadian Space Agency. We thank Fokke Creutzberg for providing high resolution photometer data and Leroy Cogger for his efforts as a PI for the CANOPUS ASI. We acknowledge NASA/GSFC, CDAWeb, and DARTS/Geotail data providers, R. Leeping (Wind MFI), L. Frank (Geotail CPI), K. Tsuruda (Geotail EFD), T. Mukai (Geotail LEP), and S. Kokubun (Geotail MGF). We thank H. Singer for providing high resolution, and CDAWeb, GOES 8 and GOES 9 data. Poste-de-la-Baleine and Ottawa magnetic stations are funded and operated by The Geological Survey of Canada, a department of National Resources of Canada. The data of the station Bear Island that belongs to the IMAGE magnetometer network is provided by the University of Tromso, but we

would like to extend our thanks to all institutes providing magnetic data for the IMAGE, and IMAGE website providers, for an excellent site and great service. We thank Magdalena Jankowska for her efforts in creating new CANOPUS software used for this paper. This research was supported by the Natural Sciences and Engineering Research Council of Canada (NSERC) and the Canadian Space Agency.

[55] Arthur Richmond thanks Hannu E. Koskinen and another reviewer for their assistance in evaluating this paper.

References

Aikio, A. T., V. A. Sergeev, M. A. Shukhtina, L. I. Vagina, V. Angelopoulos, W. Baumjohann, and G. D. Reeves, Characteristics of pseudobreakups and substorms observed in the ionosphere, at the geosynchronous orbit, and in the tail, *J. Geophys. Res.*, *104*, 12,263, 1999.

Akasofu, S.-I., *Physics of Magnetospheric Substorms*, 599 pp., D. Reidel, Norwell, Mass., 1977.

Angelopoulos, V., W. Baumjohann, C. F. Kennel, F. V. Coroniti, M. G. Kivelson, R. Pellat, R. J. Walker, H. Lühr, and G. Paschmann, Bursty bulk flows in the inner central plasma sheet, *J. Geophys. Res.*, *97*, 4027, 1992.

Angelopoulos, V., C. F. Kennel, F. V. Coroniti, R. Pellat, M. G. Kivelson, R. J. Walker, C. T. Russel, W. Baumjohann, W. C. Feldman, and J. T. Gosling, Statistical characteristics of bursty bulk flow events, *J. Geophys. Res.*, *99*, 21,257, 1994.

Baker, D. N., and R. L. McPherron, Extreme energetic particle decreases near geostationary orbit: A manifestation of current diversion within the inner plasma sheet, *J. Geophys. Res.*, *95*, 6591, 1990.

Baker, D. N., T. I. Pulkkinen, V. Angelopoulos, W. Baumjohann, and R. L. McPherron, Neutral line model of substorms: Past results and present view, *J. Geophys. Res.*, *101*, 12,975, 1996.

Baker, D. N., T. I. Pulkkinen, J. Buchner, and A. J. Klimas, Substorms: A global instability of the magnetosphere-ionosphere system, *J. Geophys. Res.*, *104*, 14,601, 1999.

Baker, K. B., and S. Wing, A new magnetic coordinate system for conjugate studies at high latitude, *J. Geophys. Res.*, *94*, 9139, 1989.

Baumjohann, W., M. Hesse, S. Kokubun, T. Mukai, T. Nagai, and A. A. Petrukovich, Substorm dipolarization and recovery, *J. Geophys. Res.*, *104*, 24,995, 1999.

Birn, J., and M. Hesse, Details of current disruption and diversion in simulations of magnetotail dynamics, *J. Geophys. Res.*, *101*, 15,345, 1996.

Birn, J., M. Hesse, G. Haerendel, W. Baumjohann, and K. Shiokawa, Flow braking and substorm current wedge, *J. Geophys. Res.*, *104*, 19,895, 1999.

Erickson, G. M., N. C. Maynard, W. J. Burke, G. R. Wilson, and M. A. Heinemann, Electromagnetics of substorm onsets in the near-geosynchronous plasma sheet, *J. Geophys. Res.*, *105*, 25,265, 2000.

Fairfield, D. H., et al., Earthward flow bursts in the inner magnetotail and their relation to auroral brightening, AKR intensifications, geosynchronous particle injections and magnetic activity, *J. Geophys. Res.*, *104*, 335, 1999.

Frank, L. A., J. B. Sigwarth, W. R. Paterson, and S. Kokubun, Two encounters of the substorm onset region with the Geotail spacecraft, *J. Geophys. Res.*, *106*, 5811, 2001a.

Frank, L. A., W. R. Paterson, J. B. Sigwarth, and T. Mukai, Observations of plasma sheet dynamics earthward of the onset region with the Geotail spacecraft, *J. Geophys. Res.*, *106*, 18,823, 2001b.

Friedrich, E., J. C. Samson, I. Voronkov, and G. Rostoker, Dynamics of the substorm expansive phase, *J. Geophys. Res.*, *106*, 13,145, 2001a.

Friedrich, E., J. C. Samson, and I. Voronkov, Ground-based observations and plasma instabilities in auroral substorms, *Phys. Plasmas*, *8*, 1104, 2001b.

Haerendel, G., Disruption, ballooning or auroral avalanche—On the cause of substorms, in *Substorms-1, Proceedings of the First International Conference on Substorms (ICS-1)*, *Eur. Space Agency Spec. Publ.*, *SP-335*, 417, 1992.

Hones, E. W., Jr., Transient phenomena in the magnetotail and their relation to substorms, *Space Sci. Rev.*, *23*, 393, 1979.

Hones, E. W., Jr., Plasma sheet behavior during substorms, in *Magnetic Reconnection in Space and Laboratory Plasmas*, *Geophys. Monogr. Ser.*, vol. 30, edited by E. W. Hones Jr., p. 178, AGU, Washington, D. C., 1984.

Ieda, A., S. Machida, T. Mukai, Y. Saito, T. Yamamoto, A. Nishida, T. Terasawa, and S. Kokubun, Statistical analysis of the plasmoid evolution with Geotail observations, *J. Geophys. Res.*, *103*, 4453, 1998.

Ieda, A., D. H. Fairfield, T. Mukai, Y. Saito, T. Yamamoto, S. Kokubun, K. Liou, C.-I. Meng, G. K. Parks, and M. J. Brittnacher, Plasmoid ejection and auroral brightenings, *J. Geophys. Res.*, *106*, 3845, 2001.

Kaufmann, R. L., Substorm currents: Growth phase and onset, *J. Geophys. Res.*, *92*, 7471, 1987.

Koskinen, H. E. I., R. E. Lopez, R. J. Pellinen, T. I. Pulkkinen, D. N. Baker, and Bösinger, Pseudobreakup and substorm growth phase in the ionosphere and magnetosphere, *J. Geophys. Res.*, *98*, 5801, 1993.

Liou, K., C.-I. Meng, A. T. Y. Lui, P. T. Newell, M. Brittnacher, G. Parks, G. D. Reeves, R. R. Anderson, and K. Yumoto, On relative timing in substorm onset signatures, *J. Geophys. Res.*, *104*, 22,807, 1999.

Liou, K., C.-I. Meng, P. T. Newell, K. Takahashi, S.-I. Ohtani, A. T. Y. Lui, M. Brittnacher, and G. Parks, Evaluation of low-latitude Pi2 pulsations as indicators of substorm onset using Polar ultraviolet imagery, *J. Geophys. Res.*, *105*, 2495, 2000.

Lui, A. T. Y., A synthesis of magnetospheric substorm models, *J. Geophys. Res.*, *96*, 1849, 1991.

Lui, A. T. Y., R. E. Lopez, S. M. Krimigis, R. W. McEntire, L. J. Zanetti, and T. A. Potemra, A case study of magnetotail current sheet disruption and diversion, *Geophys. Res. Lett.*, *7*, 721, 1988.

Lyons, L. R., A new theory for magnetospheric substorms, *J. Geophys. Res.*, *100*, 19,069, 1995.

Lyons, L. R., G. T. Blanchard, J. C. Samson, R. P. Lepping, T. Yamamoto, and T. Moretto, Coordinated observations demonstrating external substorm triggering, *J. Geophys. Res.*, *102*, 27,039, 1997.

Maynard, N. C., W. J. Burke, E. M. Basinska, G. M. Erickson, W. J. Hughes, H. J. Singer, A. G. Yahnin, D. A. Hardy, and F. S. Mozer, Dynamics of the inner magnetosphere near times of substorm onsets, *J. Geophys. Res.*, *101*, 7705, 1996.

McPherron, R. L., Growth phase of magnetospheric substorms, *J. Geophys. Res.*, *75*, 5592, 1970.

McPherron, R. L., Is there a near-Earth neutral line?, in *Substorms-1, Proceedings of the First International Conference on Substorms (ICS-1)*, *Eur. Space Agency Spec. Publ.*, *SP-335*, 417, 1992.

Mishin, V. M., C. T. Russel, T. I. Saifudinova, and A. D. Bazarzhapov, Study of weak substorms observed during December 8, 1990. Geospace Environment Modeling campaign: Timing of different types of substorm onsets, *J. Geophys. Res.*, *105*, 23,263, 2000.

Miyashita, Y., S. Machida, T. Mukai, Y. Saito, K. Tsuruda, H. Hayakawa, and P. R. Sutcliffe, A statistical study of variations in the near and mid-distant magnetotail associated with substorm onset: GEOTAIL observations, *J. Geophys. Res.*, *105*, 15,913, 2000.

Murphree, J. S., and M. L. Johnson, Clues to plasma processes based on Freja UV observations, *Adv. Space Res.*, *18*, 95, 1996.

Nagai, T., M. Fujimoto, Y. Saito, S. Machida, T. Terasawa, R. Nakamura, T. Yamamoto, T. Mukai, A. Nishida, and S. Kokubun, Structure and dynamics of magnetic reconnection for substorm onsets with Geotail observations, *J. Geophys. Res.*, *103*, 4419, 1998.

Nakamura, R., D. N. Baker, T. Yamamoto, R. D. Belian, E. A. Bering III, J. R. Benbrook, and J. R. Theall, Particle and field signatures during pseudobreakup and major expansion onset, *J. Geophys. Res.*, *99*, 207, 1994.

Nakamura, R., W. Baumjohann, M. Brittnacher, V. A. Sergeev, M. Kubyshkina, T. Mukai, and K. Liou, Flow bursts and auroral activations: Onset timing and foot point location, *J. Geophys. Res.*, *106*, 10,777, 2001a.

Nakamura, R., W. Baumjohann, R. Schödel, M. Brittnacher, V. A. Sergeev, M. Kubyshkina, T. Mukai, and K. Liou, Earthward flow bursts, auroral streamers, and small expansions, *J. Geophys. Res.*, *106*, 10,791, 2001b.

Ohtani, S., K. Takahashi, L. J. Zanetti, T. A. Potemra, R. W. McEntire, and T. Iijima, Initial signatures of magnetic field and energetic particle fluxes at tail reconfiguration: Explosive growth phase, *J. Geophys. Res.*, *97*, 19,311, 1992.

Ohtani, S., F. Creutzberg, T. Mukai, H. Singer, A. T. Y. Lui, M. Nakamura, P. Prikryl, K. Yumoto, and G. Rostoker, Substorm onset timing: The December 31, 1995 event, *J. Geophys. Res.*, *104*, 22,713, 1999.

Opgenoorth, H. J., M. A. L. Persson, T. I. Pulkkinen, and R. J. Pellinen, Recovery phase of magnetospheric substorm and its association with morning-sector aurora, *J. Geophys. Res.*, *99*, 4115, 1994.

Pellinen, R. J., and W. J. Heikkila, Observations of auroral fading before breakup, *J. Geophys. Res.*, *83*, 4207, 1978.

Petrukovich, A. A., et al., Two spacecraft observations of a reconnection pulse during an auroral breakup, *J. Geophys. Res.*, *103*, 47, 1998.

Pulkkinen, T. I., D. N. Baker, L. L. Cogger, L. A. Frank, J. B. Sigwarth, S. Kokubun, T. Mukai, H. J. Singer, J. A. Slavin, and L. Zelenyi, Spatial extent and dynamics of a thin current sheet during the substorm growth phase on December 10, 1996, *J. Geophys. Res.*, *104*, 28,475, 1999.

Reeves, G. D., G. Kettmann, T. A. Fritz, and R. D. Belian, Further investigation of the CDW 7 substorm using geosynchronous particle data: Multiple injections and their implications, *J. Geophys. Res.*, *97*, 6417, 1992.

Rostoker, G., On the place of the pseudo-breakup in a magnetospheric substorm, *Geophys. Res. Lett.*, *25*, 217, 1998.

Rostoker, G., The evolving concept of a magnetospheric substorm, *J. Atmos. Terr. Phys.*, *61*, 85, 1999.

Rostoker, G., S.-I. Akasofu, J. Foster, R. A. Greenwald, Y. Kamide, K. Kawasaki, A. T. Y. Lui, R. L. McPherron, and C. T. Russell, Magne-

tospheric substorms—Definition and signatures, *J. Geophys. Res.*, *85*, 1663, 1980.

Rostoker, G., J. C. Samson, F. Creutzberg, T. J. Hughes, D. R. McDiarmid, A. G. McNamara, A. Vallance Jones, D. D. Wallis, and L. L. Cogger, CANOPUS—A ground based instrument array for remote sensing the high latitude ionosphere during the ISTP/GGS Program, in *The Global Geotail Mission*, edited by C. T. Russel, p. 743, Kluwer Acad., Norwell, Mass., 1995.

Roux, A., S. Perraut, P. Robert, A. Morane, A. Pedersen, A. Korth, G. Kremser, B. Aparicio, D. Rodgers, and R. Pellinen, Plasma sheet instability related to the westward travelling surge, *J. Geophys. Res.*, *96*, 17,697, 1991.

Samson, J. C., Mapping substorm intensifications from the ionosphere to the magnetosphere, in *SUBSTORM-2, International Conference on Substorms-2*, edited by J. R. Kan, J. D. Craven, and S.-I. Akasofu, p. 237, Univ. of Alaska, Fairbanks, 1994.

Samson, J. C., L. R. Lyons, P. T. Newell, F. Creutzberg, and B. Xu, Proton aurora and substorm intensifications, *Geophys. Res. Lett.*, *19*, 2167, 1992.

Samson, J. C., R. Rankin, and I. Voronkov, Field line resonances, auroral arcs, and substorm intensifications, in *Geospace Mass and Energy Flow: Results From the International Solar-Terrestrial Physics Program*, *Geophys. Monogr. Ser.*, vol. 104, edited by J. L. Horwitz et al., p. 161, AGU, Washington, D. C., 1998.

Samson, J. C., E. F. Donovan, and I. O. Voronkov, *CANOPUS-2000. Canada's Window on Space. A Proposal to the Canadian Space Agency on Behalf of The Canadian Space Science Community*, 46 pp., 2000.

Sergeev, V. A., P. Tanskanen, K. Mursula, A. Korth, and R. C. Elphic, Current sheet thickness in the near-Earth plasma sheet during substorm growth phase, *J. Geophys. Res.*, *95*, 3819, 1990.

Sergeev, V. A., V. Angelopoulos, D. G. Mitchell, and C. T. Russell, In situ observations of magnetotail reconnection prior to the onset of a small substorm, *J. Geophys. Res.*, *100*, 19,121, 1995.

Shiokawa, K., W. Baumjohann, and G. Haerendel, Braking of high-speed flows in the near-Earth tail, *Geophys. Res. Lett.*, *10*, 1179, 1997.

Shiokawa, K., et al., High-speed flow, substorm current wedge, and multiple Pi 2 pulsations, *J. Geophys. Res.*, *103*, 4491, 1998.

Tsyganenko, N. A., A magnetospheric magnetic field model with a warped tail current sheet, *Planet. Space Sci.*, *37*, 5, 1989.

Voronkov, I., E. Friedrich, and J. C. Samson, Dynamics of the substorm growth phase as observed using CANOPUS and SuperDARN instruments, *J. Geophys. Res.*, *104*, 28,491, 1999.

Voronkov, I., E. F. Donovan, B. J. Jackel, and J. C. Samson, Large-scale vortex dynamics in the evening and midnight auroral zone: Observations and simulations, *J. Geophys. Res.*, *105*, 18,505, 2000a.

Voronkov, I., J. C. Samson, E. Friedrich, R. Rankin, V. T. Tikhonchuk, and E. F. Donovan, On the distinction between, and relevance of, auroral breakup and substorm expansive phase onset, in *Substorms-5, Proceedings of the 5th International Conference on Substorms (ICS-5)*, *Eur. Space Agency Spec. Publ.*, *SP-443*, 249, 2000b.

Yahnin, A. G., Observational constraints on the plasma sheet processes related to auroral breakup, in *Substorms-5, Proceedings of the 5th International Conference on Substorms (ICS-5)*, *Eur. Space Agency Spec. Publ.*, *SP-443*, 263, 2000.

E. F. Donovan, Department of Physics and Astronomy, University of Calgary, Calgary, Alberta, Canada, T2N 1N4. (donovan@phys.ucalgary.ca; jackel@phys.ucalgary.ca)

J. C. Samson and I. O. Voronkov, Department of Physics, University of Alberta, Edmonton, Alberta, Canada, T6G 2J1. (samson@space.ualberta.ca; igor@space.ualberta.ca)